J. Synchrotron Rad. (1998). **5**, 202–207

Advanced Capabilities for Future Light Sources

Kwang-Je Kim
Lawrence Berkeley National Laboratory, USA. E-mail: kwangje@lbl.gov

(*Received 1 September 1997; accepted 7 January 1998*)

Methods to extend the capabilities of light sources beyond those available at the current generation synchrotron radiation sources based on undulators in electron storage rings are discussed. Taking advantage of the radiation–particle interaction and/or the availability of high-power ultrashort optical lasers, it is possible to develop sources with higher brightness, smaller temporal resolution, or higher photon energy. This paper is a summary of some of these schemes, with an emphasis on new ideas rather than on a comprehensive review.

Keywords: future light sources.

1. Introduction

The state-of-the-art light sources, also known as third-generation sources, provide time-averaged spectral brightness approaching 10^{21} photons s^{-1} mm^{-2} mrad^{-2} (0.1% spectral bandwidth)$^{-1}$, up to about 10 keV photon energy, the radiation consisting of 10–20 ps bursts (see, for example, Winick, 1998). They are based on spontaneous radiation from undulators, schematically illustrated in Fig. 1, placed in low-emittance high-current electron storage rings. The brightness of undulator radiation is much higher than that of a bending-magnet source due to interference of radiation from different parts along the length of the undulator (for a review, see Kim, 1989).

The wavelength λ of the undulator radiation is given by the difference in the average forward distances traveled by the light and the electron in one undulator period:

$$\lambda = \lambda_u(1 - \bar{\beta}_z) = \frac{1 + K^2/2}{2\gamma^2}\lambda_u. \qquad (1)$$

Here λ_u is the period of the undulator magnet, $\bar{\beta}_z$ is the average forward speed of the electron divided by the speed of light, γ is the Lorentz factor of electron motion, and K is such that K/γ is the maximum deflection angle of the sinusoidal electron trajectory.

Undulator radiation is an incoherent sum of radiation from individual electrons. Therefore, the total radiation phase space of undulator radiation is given by a convolution of the coherent radiation phase space of individual electrons and the electron-beam phase space. Since the electron-beam phase-space area is characterized by the r.m.s. emittance ε_x, and the corresponding quantity for coherent radiation is $\lambda/4\pi$, where λ is the radiation wavelength, undulator radiation becomes maximally bright when

$$\varepsilon_x \leq \lambda/4\pi. \qquad (2)$$

In this case the undulator radiation becomes transversely coherent, thus permitting interference techniques such as holography. For a typical third-generation light source, the coherence condition is satisfied for radiation wavelengths longer than 100 Å.

Light sources with enhanced performance are possible within the framework of the spontaneous radiation from electron storage rings: larger circumference rings and/or in-vacuum micro-undulators could be employed for higher brightness and/or higher photon energy; quasi-isochronous rings may provide shorter time resolution, *etc*. These topics have been reviewed extensively (see, for example, Winick, 1998), and will not be discussed further in this paper.

Normally, the interaction of the radiation beam with the electron beam in an undulator is negligible. However, such interaction does exist and may be referred to as the free-electron-laser (FEL) interaction because it is the basis of FEL devices (Madey, 1971). Up to the UV spectral range, the storage-ring-based FEL oscillators can provide spectral brightness several orders of magnitude higher than available in the third-generation light sources. However, the FEL oscillators are limited in spectral coverage due to the absence of high-reflectivity mirrors for short-wavelength radiation.

For sufficiently good beam qualities and long undulators, the spontaneous undulator radiation generated at the beginning can be amplified through the FEL interaction to a very high power radiation, fully coherent transversely and quasi-coherent temporally (Bonifacio *et al.*, 1985; Kim, 1986; Wang & Yu, 1986). Such radiation is called the self-amplified spontaneous emission (SASE) and is the basis of several proposals based on the recent developments in high-brightness high-energy electron linacs. The SASE is at the moment the only known route to an intense coherent tunable source for wavelengths down to 1 Å. This will be the subject of §2.

The recent developments in high-power ultrashort optical lasers based on chirped pulse amplification techniques (Strickland & Mourou, 1985; and for a review, see

Perry & Mourou, 1994) offer new opportunities for the next generation of light sources *via* Thomson or Compton scattering with the electron beam or heavy-ion beam. A general discussion of this topic is given in §3.

Two methods of generating ultrashort X-ray pulses, with pulse lengths of about 100 fs, are discussed in §4. The first is the Thomson scattering of a low-energy electron beam (about 50 MeV) with ultrashort optical pulses in a 90° scattering configuration (Kim *et al.*, 1994). The other is to 'slice out' an ultrashort portion of an electron beam based on the FEL interaction (Zholents & Zolotorev, 1996).

Scattering of a high-power laser beam by a particle beam could lead to cooling of the particle beam, and hence higher brightness for the scattered radiation. This fact can be used to design compact low-energy (about 10 MeV) electron storage rings for generation of X-rays (Huang & Ruth, 1997), or to cool the high-energy electron beams in linacs (Telnov, 1997). Another example is the radiative cooling in a relativistic heavy-ion ring, which has the possibility of generating intense, 100 keV photon beams which are diffraction limited (Bessonov & Kim, 1996). This is the subject of §5.

For extremely high energies, photons of TeV quantum energy could be generated by scattering laser beams with the TeV electron beams in a linear collider to produce gamma–gamma collisions for elementary particle physics (Telnov, 1995). This ultimate photon energy frontier is discussed in §6.

Conclusions are given in §7 of the paper.

2. Free-electron lasers (FELs)

2.1. *FEL interaction*

In general it is difficult to maintain a sustained interaction of a fully propagating short-wavelength radiation beam with an electron beam, because light moves faster than electrons and, furthermore, the electric field is transverse to the propagation direction. However, the interaction becomes possible within an undulator. There the electron and the radiation beam can exchange energy due to the electron's transverse motion. Furthermore, if the radiation wavelength satisfies equation (1), the radiation beam moves exactly one wavelength ahead of the electron beam as the latter moves along one undulator period. Because of the periodicity of the system, the interaction is then maintained through the entire length of the undulator.

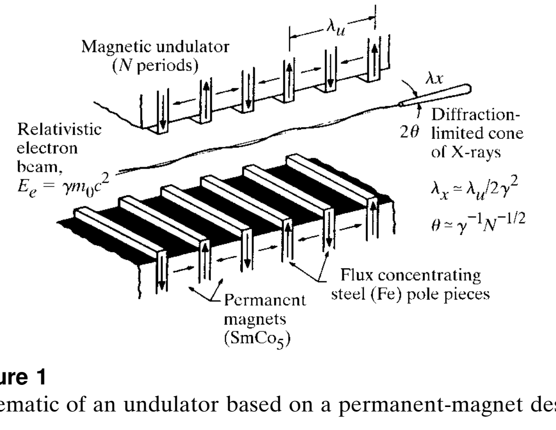

Figure 1
Schematic of an undulator based on a permanent-magnet design.

The resonant (sustained) interaction of the electron and the radiation beam explained above will be referred to as the FEL interaction.

The FEL interaction causes periodic energy modulation with period λ in the electron beam. The energy modulation evolves to a density modulation due to the energy dependence of the axial velocity in the undulator, and hence leads to a 'stimulated' emission at the same wavelength λ. This provides the amplification mechanism, which is the basic operating principle of FEL devices (Madey, 1971).

The FELs, which can be based either on linacs or storage rings, are more versatile than atomic or molecular lasers in that the wavelength can be chosen arbitrarily by choosing a suitable electron-beam energy and the strength of the undulator magnetic field. However, it is necessary that the electron-beam emittance should be small to satisfy equation (2).

2.2. *FEL oscillator*

When the amplification is low, an oscillator configuration may be formed by placing two mirrors, separated by half of the electron bunch spacing, at both ends of the undulator. The undulator radiation pulses from the initial electron bunches interact with the subsequent bunches, increasing the intensity and the coherence from pass to pass, until the intra-cavity intensity reaches the saturation level. Such an arrangement is known as an FEL oscillator and produces highly coherent radiation beams with brightness many orders of magnitude higher than that of the undulator radiation.

Storage-ring-based FELs have been successfully operated for user experiments at SuperACO and at other laboratories (for a review, see Couprie, 1997). However, the operation of FEL oscillators has been limited to UV or longer wavelengths; the shortest wavelength limit for an FEL oscillator to date has been 2400 Å at Novosibirsk (Drobyazko *et al.*, 1989), the limiting factor being the availability of mirrors.

2.3. *High-gain FEL amplifier and self-amplified spontaneous emission (SASE) for X-rays*

With suitably high electron-beam brightness and a long undulator, the amplification in a single pass may be sufficiently high that the FEL can be operated in an amplifier mode, thus obviating the need for high-reflectivity mirrors. If seed lasers are available, the FEL can amplify the input radiation at the fundamental or at higher harmonic wavelengths (Yu, 1991). However, the seeded high-gain amplifier cannot generate X-rays due to the spectral limit of the seed lasers.

If the amplification is extremely high, about 10^7–10^8, then the spontaneous undulator radiation in the beginning part of the undulator can be amplified to an intense radiation, referred to as SASE (Bonifacio *et al.*, 1985; Kim, 1986; Wang & Yu, 1986). The radiation is fully coherent transversely. Temporally, the spectral bandwidth is typically about 0.1%. Since it is limited neither by the availability of mirrors nor by seed lasers, SASE is currently the only known approach for obtaining tunable coherent radiation down to 1 Å wavelength, with brightness much higher than that available at the current third-generation synchrotron radiation facilities.

Several experimental projects are either in progress or being planned in laboratories around the world, some of which are listed in Fig. 2. As indicated in the figure, the proof-of-principle experiments for wavelengths longer than 10 µm have already demonstrated a significant level of single pass gain as well as the start-up from noise. In the mid-infrared region ($\lambda \simeq 5$ µm), the CLIO group has also found evidence of noise start-up and amplification (Prazeres *et al.*, 1997). The experiments at APS (Milton, 1997) and DESY (Rossbach *et al.*, 1995), at a wavelength around 1000 Å, are planned to be carried out within 1–2 years.

Eventually the goal is to achieve SASE at X-ray wavelengths, for which the only linac available to date is the SLAC linac (Pellegrini, 1992). The project is called the Linear Coherent Light Source (LCLS) (Cornacchia *et al.*, 1997). In this project, a laser-driven RF photocathode gun (Sheffield, 1989) with an emittance correction scheme (Carlsten, 1989) produces electron bunches, each with a charge of 1 nC, normalized emittance $\gamma\varepsilon_x$ of about 1×10^{-6} m rad, and a pulse length of about 10 ps. The bunches are compressed to about 100 fs to increase the peak current to about 3.5 kA, and accelerated to high energy (10–20 GeV). It is important to prevent emittance dilution during the acceleration, using techniques developed for linear-collider R&D (for a review, see Loew, 1995). Also, the error in the undulator magnetic field needs to be controlled tightly. The peak spectral brightness (during the 100 fs pulse length) of the LCLS would be more than ten orders of magnitude higher than that of the undulator radiation from third-generation synchrotron radiation sources. In addition, the pulse length is about a hundred times shorter, thereby improving the time resolution by the same factor. The enhancement of the average brightness is less, due to the smaller repetition rate of the linac. However, the average spectral brightness of LCLS is still 3–4 orders of magnitude higher than that of the undulator sources. It can be increased further by increasing the bunch repetition rate if a superconducting linac is used, as proposed at DESY, permitting multi-user operation as in the storage-ring-based sources (Brinkman *et al.*, 1997).

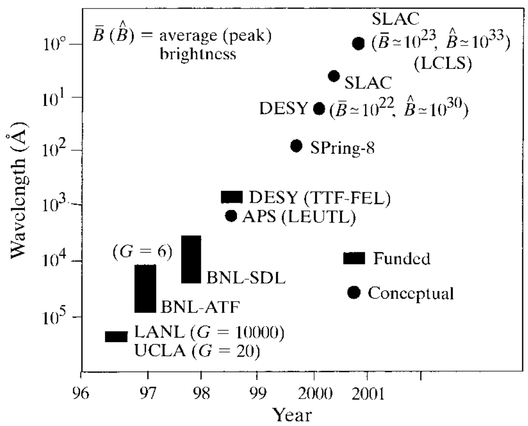

Figure 2
SASE projects around the world. G = the experimentally observed gain to date.

3. High-power solid-state laser and Compton scattering

With the invention of the chirped pulse amplification (CPA) concept – a technique for avoiding non-linear effects in high-gain amplifiers by stretching a short laser pulse to a long pulse before amplification – compact solid-state lasers producing ultrashort optical pulses (10–100 fs) with a pulse energy of about 1 J have been developed for practical use during the past decade (Strickland & Mourou, 1985; for a review, see Perry & Mourou, 1994). The high electric field within such a high-power laser pulse, when combined with the particle-beam technique, gives rise to several interesting schemes for novel radiation sources.

These new sources are either based on Compton scattering (Arutyumian & Tumanian, 1963; Milburn, 1963) or on FEL interaction. Specific examples will be considered in later sections. However, the general characteristics of the Compton-scattered radiation of a laser beam with a particle beam can be summarized as follows.

The wavelength of the scattered radiation is given by:

$$\lambda_s = \frac{2n(1 + \cos\alpha)\gamma^2}{1 + \gamma^2\theta^2 + K^2/2 + nx}\lambda_L, \qquad (3)$$

where n is the harmonic number (we consider the case n = 1 in the following), λ_L is the laser wavelength, α is the angle between the incoming laser beam and the particle beam, θ is the angle between the scattered radiation and the particle beam, $K = eB_o\lambda_L/(4\pi mc^2)$, B_o = the magnetic field in the laser field, m = the particle mass, and $x = 4\gamma\hbar\omega_L/mc^2$ ($\omega_L = 2\pi c/\lambda_L$), is the recoil parameter. The power of the scattered radiation is

$$P_s = 4\sigma\cos^2(\alpha/2)\gamma^2(\mathrm{d}P_L/\mathrm{d}A), \qquad (4)$$

where σ is the scattering cross section, and $\mathrm{d}P_L/\mathrm{d}A$ is the laser power per unit area.

When the quantum recoil is negligible, $x \ll 1$, and the internal structure of the particle can be neglected, then the Compton scattering reduces to the classical Thomson scattering with cross section $\sigma = 8\pi r_o^2/3$, $r_o = e^2/mc^2$. The formula in this case for the backscattering configuration (α

= 0) reduces to equation (1), if one identifies $\lambda_s \rightarrow \lambda$ and $\lambda_L \rightarrow 2\lambda_u$.

Thomson backscattering could be the basis for a compact source of X-rays using low-energy electron beams (Sprangle *et al.*, 1992). However, the brightness of such a source is limited because the electron beam has in general low brightness at low energies.

4. Generation of femtosecond X-ray pulses

A time scale of fundamental importance in condensed matter research is about 100 fs, since this is the time scale at which chemical reactions, phase transitions and surface processes occur. Although the femtosecond (10–100 fs) optical lasers discussed in the previous section can be used for an indirect study of the atomic motion on such a time scale, a more direct probe will be femtosecond X-ray pulses exploring the time evolution of the core levels. Two techniques for generating femtosecond X-ray pulses based on the combined use of the femtosecond optical lasers and the electron-beam techniques are described below.

4.1. *90° Thomson scattering*

Thomson scattering as an X-ray generator is most efficient when the electron pulse meets the laser pulse head on (α = 0) – the backscattering configuration.

However, the duration of the scattered X-ray pulse is about the same as that of the electron pulse (assuming the latter is shorter than the former). The duration of the electron pulse length in a linac is usually about 10 ps, and it is difficult to compress it smaller than picosecond level.

However, femtosecond X-ray pulses can be generated in 90° Thomson scattering in which a low-energy electron pulse meets femtosecond optical laser pulses at a right angle (α = 90°) (Kim *et al.*, 1994). By focusing the electron beam tightly in the transverse direction to a spot size comparable with the length of the laser pulse, the scattered X-ray pulse can be made to be of femtosecond duration.

This concept has been tested experimentally with a 50 MeV electron linac and an ultrashort optical laser (λ = 0.8 μm, 100 fs duration, 1 J pulse^{-1}) producing 30 keV X-rays of 300 fs duration (Schoenlein *et al.*, 1996).

4.2. *Femto-slicing technique*

The femtosecond X-ray pulse generation based on 90° Thomson scattering described in the previous subsection is appropriate for low-energy linacs. Here another technique, called femto-slicing, will be described, which is appropriate for high-energy (~1 GeV) electron storage rings.

If a 100 fs part of the bunch could be separated from the main bunch, *i.e.*, 'sliced out', the synchrotron radiation from that part can be isolated by a mask, thus producing a 100 fs X-ray pulse. The slicing can be achieved by having an ultrashort optical laser pulse travel together with an electron bunch (typically several tens of ps) through an undulator in a straight section of a storage ring (Zholents & Zolotorev, 1996). If the undulator is tuned to the wavelength of the laser, then the thin slice of the electron beam interacting with the short laser pulse develops energy modulation *via* the FEL interaction (see Fig. 3). The laser power should be chosen so that the amplitude of the modulation is several times larger than the natural r.m.s. spread. The electrons near the top and bottom of the energy modulation are then separated spatially by passing through a dispersive section (between undulator A and bending magnet B in Fig. 3). The displaced electron-beam slice emits displaced X-rays in a synchrotron radiation device, such as bending magnet B in Fig. 3. By imaging the source to the experimental area, and by employing an aperture to transmit only the X-rays from the displaced source (Fig. 3), it is possible to provide femtosecond X-ray pulses.

The energy of the optical pulse required for femto-slicing is much less than the case for 90° Thomson scattering. Therefore the laser for femto-slicing can be run at a repetition rate higher than is possible in the case of 90° Thomson scattering, with a concomitant increase in average X-ray flux.

A proof-of-principle experiment of the femto-slicing technique is in progress at LBNL using the ALS ring.

5. Radiative laser cooling and high-brightness X- and gamma-ray beams

The key to high-brightness radiation is small particle-beam emittance. In linacs, the invariant emittance $\gamma\varepsilon_x$ is determined by the gun. At present, the best performance for an electron beam is that offered by the laser-driven RF photocathode ($\gamma\varepsilon_x \simeq$ 1–2 mm mrad for a 1 nC bunch). In the electron storage ring, the emittance is determined by the radiative cooling due to synchrotron radiation in bending magnets and quantum excitation. The value of the emittance achieved in third-generation synchrotron radiation rings is similar to that from the laser driven RF photo-cathode gun.

The radiative cooling does not take place in a linac. For a storage ring, it is not effective either at low energy ($\geq$500 MeV), because of insufficient synchrotron emission, or at high energy, due to the increased quantum excitation.

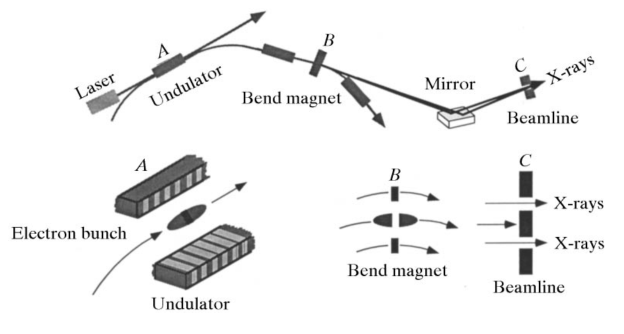

Figure 3
Schematic of the femto-slicing technique. (Courtesy of A. S. Zholents.)

It is therefore important to consider other methods for cooling particle beams.

Of several schemes to cool the particle beams (for a review, see Sessler, 1996), the radiative laser cooling of an electron beam (Telnov, 1997) and that of a non-fully stripped ion beam (Bessonov & Kim, 1996) are particularly interesting from the point of view of radiation generation: both are based on backscattering with high-power optical beams. The scattering process reduces the invariant emittance because the scattered radiation is predominantly in the direction of the particle motion.

5.1. *Radiative laser cooling of electron beams*

Radiative laser cooling of an electron beam was originally proposed for application to improve beam qualities for a TeV linear collider (Telnov, 1997). The scheme is to Thomson backscatter GeV electron beams with high-power optical beams to decelerate a significant fraction of the electron-beam energy, and then to reaccelerate.

A more gentle variant of the idea is to cool a low-energy ($<\sim$10 MeV) electron storage ring (Huang & Ruth, 1997). The laser pulse is stored in an optical cavity containing a straight section of the storage ring. As the electron beam passes through the straight section it collides head-on with the optical pulse, producing Thomson-backscattered X-rays and at the same time cooling the electron beam in the process. The usual radiative cooling due to synchrotron radiation is negligible for such a low-energy ring. The electron optics must be designed so that the interaction region in the straight section is dispersionless to minimize the quantum excitation.

5.2. *Radiative laser cooling of relativistic ion beams and generation of diffraction-limited gamma rays*

The idea here is similar to the cooling in the low-energy electron ring discussed in the previous subsection, except that the compact low-energy electron ring is replaced by a large ring storing non-fully stripped, relativistic heavy-ion beams (Bessonov & Kim, 1996). For efficient scattering, the laser wavelength must be chosen so that $\lambda_L = 2\gamma\lambda^*$, where λ^* is the wavelength corresponding to one of the transition energies of the ion in its rest frame. Equation (3) is still applicable if K and x are set to zero (due to the heavy mass of ions). Equation (4) is also applicable if the cross section σ is interpreted correctly: at exact resonance the cross section is $\sigma = \lambda^{*2}$. If the laser has a bandwidth $\Delta\lambda/\lambda_L$which is broader than the intrinsic line width ($\simeq r_o/\lambda^*$), then $\sigma \simeq \bar{\sigma} = \lambda^* r_o(\lambda_L/\Delta\lambda)$. Here $r_o = e^2/MC^2$, where M is the mass of the heavy ion. In radiative laser cooling, the laser bandwidth is chosen to be broad, to cover the Doppler bandwidth of the whole ion beam so that the laser beam interacts with all ions in the beam with an average cross section $\bar{\sigma}$. The *radiative* laser cooling discussed here is different from the well known laser cooling employing narrow bandwidth lasers.

As an example, a beam of N-like Xe ions stored in RHIC with $\gamma = 97$ can be cooled with a laser wavelength $\lambda_L = 3954$ Å, in near resonance with the transition between the states $(2S^2 2p^3)^4 S3/2$ and $(2S^2 2p^3)^4 P3/2$. With 2×10^9 ions per bunch and a bunch spacing of 224 ns, the beam can be cooled with a 100 kW laser beam consisting of 24 mJ pulses. Such high power is not available at the present time but may be achieved inside an FEL cavity.

6. Photon beams in the TeV energy range

Compton scattering of an optical laser pulse with electrons in the TeV energy range, as can be checked by equation (3), gives rise to scattered photons which are also in the TeV energy range. The high-energy gamma photon can be used for scattering with either TeV electrons or other TeV gamma photons (Telnov, 1995). Therefore, if a linear collider for e^+e^- collisions with TeV energy is constructed in the future (for a review, see Loew, 1995), it would make sense to provide a second interaction region for gamma–gamma collisions to provide alternative experiments not easily provided by e^+e^- collisions.

A schematic illustration of the interaction region of the gamma–gamma collider is shown in Fig. 4. Two electron beams of TeV energy from their representative final focus system are heading towards the interaction point (IP). At a short distance before the IP, a laser pulse is focused and Compton backscattered by electrons, resulting in a high-energy beam of photons. The photon beam follows the original electron motion within a narrow angular divergence of $1/\gamma$, and arrives at the IP in a tight focus. It collides at the IP with an opposing high-energy photon beam similarly produced by a second electron beam. By choosing the helicities of the electrons and laser photons as shown in Fig. 4, the luminosity spectrum of the gamma–gamma collider exhibits a peak with a relative FWHM width of 10–20%. The total luminosity under this peak can be made as large as 10% of the original e^+e^- luminosity. An example of a gamma–gamma collider based on the NLC design has been worked out (for a summary, see Kim, 1997).

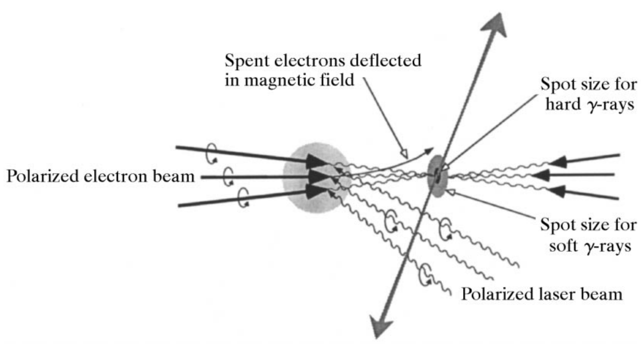

Figure 4
Schematic illustration of the conversion of TeV electrons to TeV gamma photons *via* Compton backscattering.

The gamma–gamma collider may be regarded as the ultimate energy frontier for high-brightness radiation.

7. Conclusions

The art of synchrotron radiation generation has advanced remarkably during the past decade through the development of low-emittance high-current electron storage rings, together with the development of precision magnet designs for undulators. There have also been similarly remarkable developments in linac technology, in FELs, as well as in high-power ultrashort optical lasers of compact size. It is time to take advantage of these new developments and combine them to achieve further advances in radiation-beam as well as in particle-beam capabilities. In this paper, I have discussed some specific examples of the combined techniques for generating radiation beams with higher intensity, higher spatial and temporal resolution, and/or shorter wavelength coverage, than are available in current light-source facilities.

This work was supported by the Director, Office of Energy Research, Office of High Energy and Nuclear Physics, Division of High Energy Physics, of the Department of Energy under Contract No. DE-AC 03-76SF00098.

References

Arutyumian, F. R. & Tumanian, V. A. (1963). *Phys. Lett.* **4**, 176.
Bessonov, E. G. & Kim, K.-J. (1996). *Phys. Rev. Lett.* **76**, 431.
Bonifacio, R., Pellegrini, C. & Narducci, L. M. (1985). *Opt. Commun.* **50**, 6.
Brinkman, R., Materlik, G., Rossbach, J., Schneider, J. & Wiik, B.-H. (1997). *Proc. FEL'96.*
Carlsten, B. (1989). *Nucl. Instrum. Methods A*, **285**, 313.
Cornacchia, M. *et al.* (1997). *SPIE Proc.* **2998**, 2.
Couprie, M. E. (1997). *Nucl. Instrum. Methods A*, **393**, 13.
Drobyazko, I. B. *et al.* (1989). *Nucl. Instrum. Methods A*, **282**, 424.
Huang, Z. & Ruth, R. D. (1997). *Laser Electron Storage Ring*. Report SLAC-PUB-7556. Stanford Linear Accelerator Center, USA.
Kim, K.-J. (1986). *Phys. Rev. Lett.* **57**, 1871.
Kim, K.-J. (1989). *Physics of Particle Accelerators*, AIP Conf. Proc. Vol. 184, edited by M. Month & M. Dienes, p. 565. New York: American Institute of Physics.
Kim, K.-J., Chattopadhyay, S. & Shank, C. V. (1994). *Nucl. Instrum. Methods A*, **341**, 351.
Kim, K.-J. (1997). *Nucl. Instrum. Methods A*, **393**, 530–535.
Loew, G. (1995). *International Linear Collider Technical Review Committee Report*. Report SLAC-R-95–471. Stanford Linear Accelerator Center, USA.
Madey, J. M. J. (1971). *J. Appl. Phys.* **42**, 1906.
Milburn, R. H. (1963). *Phys. Rev. Lett.* **10**, 75.
Milton, S. V. (1997). *Advanced Photon Source Low-Energy Undulator Test Line.* APS Preprint.
Pellegrini, C. (1992). In *Proc. Workshop 4th Generation Light Sources*, edited by M. Cornacchia & H. Winick. Report 92/02. Stanford Synchrotron Radiation Laboratory, USA.
Perry, M. D. & Mourou, G. (1994). *Science*, **264**, 917.
Prazeres, R. *et al.* (1997). *Phys. Rev. Lett.* **78**, 2124.
Rossbach, J. *et al.* (1995). DESY Report TESLA-FEL 95–03. DESY, Hamburg, Germany.
Schoenlein, R. W., Leemans, W. P., Chin, A. H., Volfbeyn, P., Glover, T. E., Balling, P., Zolotorev, M., Kim, K.-J., Chattopadhyay, S. & Shank, C. V. (1996). *Science*, **274**, 236–238.
Sessler, A. M. (1996). Report LBL-38278. Lawrence Berkley Laboratory, USA.
Sheffield, R. L. (1989). In *Physics of Particle Accelerators*, Vol. 184, edited by M. Month & M. Dienes, p. 1500. New York: American Institute of Physics.
Sprangle, P., Ting, A., Esarey, E. & Fisher, A. (1992). *J. Appl. Phys.* **72**, 5032.
Strickland, D. & Mourou, G. (1985). *Opt. Commun.* **56**, 219.
Telnov, V. (1995). *Nucl. Instrum. Methods A*, **355**, 3.
Telnov, V. (1997). *Phys. Rev. Lett.* **78**, 4757.
Wang, J.-M. & Yu, L.-H. (1986). *Nucl. Instrum. Methods A*, **250**, 396.
Winick, H. (1998). *J. Synchrotron Rad.* **5**, 168–175.
Yu, L.-H. (1991). *Phys. Rev. A*, **44**, 5178.
Zholents, A. A. & Zolotorev, M. S. (1996). *Phys. Rev. Lett.* **76**, 916.